ISSN 1070-3284, Russian Journal of Coordination Chemistry, 2015, Vol. 41, No. 9, pp. 555–565. © Pleiades Publishing, Ltd., 2015.
Original Russian Text © L.N. Bochkarev, Yu.E. Begantsova, V.A. Il'ichev, E.V. Baranov, G.A. Abakumov, 2015, published in Koordinatsionnaya Khimiya, 2015, Vol. 41, No. 9, pp. 515–525.

Cyclometallated Iridium(III) Complex with 2-(2,4-Difluorophenyl)pyridyl and Norbornene-Substituted Pyrazolonate Ligands and Related Electroluminescent Polymers

L. N. Bochkarev[a, b, *], Yu. E. Begantsova[a, b], V. A. Il'ichev[a, b], E. V. Baranov[a, b], and G. A. Abakumov[a, b]

[a] *G. A. Razuvaev Institute of Organometallic Chemistry, Russian Academy of Sciences, ul. Tropinina 49, Nizhni Novgorod, 603600 Russia*

[b] *Nizhni Novgorod State University, pr. Gagarina 23, Nizhni Novgorod, 603600 Russia*

**e-mail: lnb@iomc.ras.ru*

Received February 25, 2015

Abstract—New cyclometallated iridium(III) complex, NBEPzIr(Dfppy)$_2 \cdot 2CH_2Cl_2$ (**I**) (NBEPzH is 1-phenyl-3-methyl-4-(5-bicyclo[2.2.1]hept-5-en-2-yl)-5-pyrazolone, and DfppyH is 2-(2,4-difluorophenyl)pyridine), is synthesized and structurally characterized. Copolymers with carbazole and iridium-containing fragments in side chains (P1–P4) are obtained from monomer **I** by the ROMP method (ROMP is Ring-Opening Metathesis Polymerization). Their photoluminescence and electroluminescence properties are studied. Copolymers P1–P4 exhibit the green electroluminescence. The maximum current efficiency (2.60 cd/A) and power efficiency (0.63 Lm/W) are reached using emitter P3.

DOI: 10.1134/S1070328415090018

INTRODUCTION

The cyclometallated iridium(III) complexes with efficient photoluminescence (PL) and electroluminescence (EL) properties find wide use as emitting materials for organic light emitting diodes (OLED) [1]. The carbochain iridium-containing polymers exhibiting intense EL of different colors in almost the whole visible spectral range have been synthesized in the recent decade [2–4]. Unlike doped systems of the host–guest type, polymer emitters are less prone to such undesirable morphological changes as phase separation and crystallization resulting in a significant worsening or the complete loss of the EL properties. In polymers with chemically bound luminophore metal complexes, emission centers are uniformly distributed over the polymer chain, preventing their aggregation and substantially decreasing the probability of concentration quenching via the mechanism of triplet–triplet annihilation [5, 6]. The use of polymer emitters makes it possible to construct OLED devices of large surface area and flexible OLED devices using the ink-jet printing method [3, 4]. In the case of low-molecular-weight electroluminophores, it is much more difficult to fabricate emission layers of large surface area using the vacuum evaporation method. The mentioned advantages of polymer emitting materials enforce the permanent development of studies on the synthesis of novel efficient electroluminescent polymers, including metal-containing ones.

In this work, we report the synthesis of a new cyclometallated iridium(III) complex with 2-(2,4-difluorophenyl)pyridyl (Dfppy$^-$) and norbornene-substituted pyrazolonate (NBEPz$^-$) ligands, NBEPzIr(Dfppy)$_2 \cdot 2CH_2Cl_2$ (**I**), and the preparation of related iridium-containing polymers P1–P4 with the efficient PL and EL properties using the ROMP method.

EXPERIMENTAL

All procedures with easily oxidizable and hydrolyzable substances were carried out in vacuo or in argon using the standard Schlenk technique. The solvents used were thoroughly purified and degassed. The syntheses of $[Ir(Dfppy)_2(Cl)]_2$ [7]; sodium pyrazolonate (NBEPz)Na(DME) [8]; and carbazole-containing monomers, namely, 9-(5-(bicyclo[2.2.1]hept-5-en-2-ylpentyl))-9*H*-carbazole (**II**) [9], 9-(bicyclo[2.2.1]hept-5-en-2-ylmethyl)-9*H*-carbazole (**III**) [10], bicyclo[2.2.1]hept-5-en-2-yl(9*H*-carbazol-9-yl)methanone (*exo* isomer) (**IV**) [11], bicyclo[2.2.1]hept-5-en-2-yl(9*H*-carbazol-9-yl)methanone (*endo* isomer) (**V**) [11], and $(H_2IMes)(3\text{-}BrPy)_2(Cl)_2Ru{=}CHPh$ (Grubbs catalyst of the third generation) [12], were carried out using known procedures. 4,7-Diphenyl-1,10-phenanthroline (BATH) and tris(8-hydroxyquinolinato)aluminum (Alq_3) (Aldrich) were used without additional purification.

^1H and $^{13}C\{1H\}$ NMR spectra were recorded on Bruker DPX-200 (^1H NMR: 200 MHz, ^{13}C NMR: 50 MHz) and Bruker Avance III-400 (^1H NMR: 400 MHz, ^{13}C NMR: 100 MHz) spectrometers. Signal assignment was performed using 2D gradient spec-

troscopy: proton–proton correlation (GE-COSY) and proton–carbon correlation (GE-HSQC). Chemical shifts are indicated in ppm relative to tetramethylsilane used as an internal standard.

IR spectra were recorded on an FSM 1201 FT-IR spectrometer. A sample of compound **I** was prepared by pellet pressing with the substance to KBr ratio equal to 1 : 200. Samples of polymers P1–P4 were prepared as thin films between KBr plates.

The molecular weight distribution of the polymers was determined by gel permeation chromatography on a Knauer chromatograph with a Smartline RID 2300 differential refractometer as a detector equipped with a set of two Phenomenex columns (Phenogel sorbent with a pore size of 10^4 and 10^5 Å, THF as an eluent, 2 mL/min, 40°C). The columns were calibrated by 13 polystyrene standards.

Electronic absorption spectra of the iridium-containing polymers in a CH_2Cl_2 solution were recorded on a PerkinElmer Lambda 25 spectrometer. Photoluminescence spectra were obtained on a PerkinElmer LS 55 fluorescence spectrometer. The relative quantum yields of polymer products P1–P4 were determined at room temperature in degassed solutions of CH_2Cl_2 at an excitation wavelength of 360 nm. The quantum yields were calculated relative to Rhodamine 6G in ethanol ($\Phi f = 0.95$) [13] using a described procedure [14].

Differential scanning calorimetry was carried out on a DSC 204 F1 Phoenix instrument (Netzsch) in a dry argon flow (flow rate 20 cm^3/min, heating rate 5°C/min). Thermogravimetric analysis was carried out with a PerkinElmer PYRIS 6 TGA thermogravimeter in a dry nitrogen flow (flow rate 80 cm^3/min, heating rate 5°C/min).

Electroluminescence spectra, current density-voltage and luminance-voltage characteristics, and the CIE chromaticity coordinates were obtained on model OLED devices without encapsulation using an automated complex conjugated with a computer and including a GW INSTEK PPE-3323 power source, a GW INSTEK GDM-8246 digital multimeter, and an Ocean Optics USB 2000 spectrofluorimeter.

Synthesis of NBEPzIr(Dfppy)$_2$ · 2CH$_2$Cl$_2$ (I). A solution of (NBEPz)Na(DME) (0.15 g, 0.37 mmol) in DME (5 mL) was added to a solution of $(Ir(Dfppy)_2Cl)_2$ (0.23 g, 0.189 mmol) in DME (15 mL) under an argon atmosphere. The reaction mixture was refluxed with a reflux condenser for 16 h, cooled to room temperature, and filtered. After the solvent was replaced by CH_2Cl_2, a yellow solution was separated from a colorless precipitate using centrifugation. The slow evaporation of the solvent at room temperature gave complex **I** in a yield of 0.33 g (85%) as yellow crystals stable in air.

IR (KBr; ν, cm^{-1}): 3051, 3041, 1095, 1063, 1031, 1004 ν, 855 $\gamma(C_{Ar}–H)$; 2929 ν, 1397 δ_s, 1311, 1157 $\delta(C_{Alk}–H)$; 1603 $\nu_{as}(C\cdots O)$; 1595 ν, 1498 ν_{as}, 1475 ν, 1264 $\nu(C=C_{Ar})$; 1527, 1452, 1399 ν(pyrazole ring); 1263, 1154 ν(C–F); 908, 876 ν(C–C); 701, 630 δ, 618 ν(chelate ring); 512, 487, 465 ν(Ir–O).

According to the data of NMR spectroscopy, complex **I** is a mixture of *endo* and *exo* isomers.

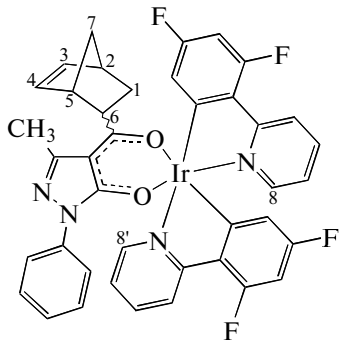

***Endo* isomer (66%).** ^{1}H NMR ($CDCl_3$; δ, ppm): 8.41 (d, $J = 5.7$ Hz, 1 H, H^8), 8.34 (d, $J = 5.6$ Hz, 1 H, $H^{8'}$), 8.17 (m, 2 H, Ar), 7.68 (m, 4 H, Ar), 7.18–6.96 (m, 5 H, Ar), 6.32 (m, 2 H, Ar), 5.68 (m, 2 H, Ar), 5.45 (dd, $J = 5.6$ and 2.4 Hz, 1 H, H^3), 5.35 (dd, $J = 5.4$ and 2.6 Hz, 1 H, H^4), 3.45 (m, 1 H, H^6), 2.81 (br.s, 1 H, H^5), 2.68 (br.s, 1 H, H^2), 2.44 (s, 3 H, Me), 1.83 (m, 1 H, H^1), 1.57 and 1.31 (both m, 2 H, H^7 and $H^{7'}$), 0.79 (m, 1 H, $H^{1'}$).

***Exo* isomer (34%).** ^{1}H NMR ($CDCl_3$; δ, ppm): 8.50 (d, $J = 5.7$ Hz, 1 H, H^8), 8.25 (d, $J = 5.3$ Hz, 1 H, $H^{8'}$), 7.80–6.20 (m, 13 H, Ar), 6.13–5.99 (m, 2 H, Ar), 5.45 (m, 2 H, H^3, and H^4), 2.93 (br.s, 2 H, H^2 and H^5), 2.33 (s, 3 H, Me), 2.21–0.68 (m, 5 H, H^1, $H^{1'}$, H^6, H^7, and $H^{7'}$).

All isomers. ^{13}C ($CDCl_3$; δ, ppm): 194.3, 192.2, 165.6, 165.3, 165.1, 163.8, 163.7, 162.0, 161.9, 161.4, 161.32, 161.26, 161.19, 161.15, 159.4, 159.3, 150.0, 149.2, 148.9, 148.8, 148.4, 148.3, 148.2, 148.0, 147.7, 147.6, 139.1, 138.2, 138.1, 138.0, 137.1, 136.1, 135.8, 134.7, 134.1, 130.0, 128.6, 128.4, 124.4, 122.5, 122.3, 122.1, 121.7, 121.6, 119.5, 115.5, 115.4, 115.2, 115.1, 105.9, 105.5, 53.4, 50.0, 49.8, 49.6, 48.1, 47.8, 47.4, 46.7, 46.3, 46.2, 44.9, 43.2, 42.4, 41.9, 41.8, 32.5, 31.4, 29.7, 28.9, 28.3, 18.1, 17.8.

For $C_{42}H_{33}N_4O_2F_4Cl_4Ir$		
anal. calcd., %:	C, 48.70;	H, 3.21.
Found, %:	C, 48.63;	H, 3.30.

Synthesis of copolymer P1. The Grubbs catalyst of the third generation (0.0025 g, 0.0030 mmol) in CH_2Cl_2 (3 mL) was added to a mixture of monomers **I** (0.0340 g, 0.0328 mmol) and **II** (0.0833 g, 0.2979 mmol) in CH_2Cl_2 (5 mL). The mixture was stirred at room temperature. The reaction course was

monitored by thin layer chromatography (TLC). After the end of copolymerization (2.5 h), several droplets of ethyl vinyl ether were added to the reaction mixture to decompose the catalyst, and the mixture was additionally stirred for 20 min. A copolymer formed was precipitated with methanol, additionally purified by reprecipitation with methanol from CH_2Cl_2, and dried in vacuo at room temperature to a constant weight. The yield of copolymer P1 as a yellow powder was 0.11 g (90%).

IR (ν, cm^{-1}): 3051, 3021, 1074, 1021, 1003 δ, 852 γ(C_{Ar}–H); 2929 ν, 1402 δ_s(C_{Alk}–H); 2852 ν, 1462, 724 δ(CH_2); 1604, 1376 ν(C···O); 1600, 1482, 1231 ν(C=C_{Ar}); 1577, 1536 ν(pyrazole ring); 1263, 1154 ν(C–F); 970 δ(C=C), 748 δ(C=C–H); 704 δ, 618 ν(chelate ring); 512, 497 ν(Ir–O). ^{1}H NMR ($CDCl_3$; δ, ppm): 7.98 (m, 18H, Ar), 7.29 (m, 42 H, Ar), 7.10 (m, 21 H, Ar), 5.11 (m, 20 H), 4.12 (m, 12 H), 0.6–3.0 (m, 132 H).

For $C_{232}H_{245}N_{12}O_2F_4Ir$		
anal. calcd., %:	C, 79.56;	H, 7.07.
Found, %:	C, 79.46;	H, 7.12.

M_w = 24800, M_n = 14300, M_w/M_n = 1.7, T_g = 89.0°C, T_d = 332°C (at 5% mass loss).

Synthesis of P2 from compounds **I** (0.0389 g, 0.0375 mmol) and **III** (0.0819 g, 0.2995 mmol) was similar to the procedure described for P1. The copolymerization time was 2 h. The yield was 0.11 g (91%).

IR (ν, cm^{-1}): 3051, 3021 ν, 1071, 1021, 1003 δ, 852 γ(C_{Ar}–H); 2929 ν, 1402 δ_s(C_{Alk}–H); 2864 ν, 1462 δ(CH_2); 1604, 1379 ν(C···O); 1601, 1482 ν(C=C_{Ar}); 1577, 1536 ν(pyrazole ring); 1263, 1154 ν(C–F); 973 δ(C=C), 748 δ(C=C–H); 704 δ, 618 ν(chelate ring); 512, 464 ν(Ir–O). ^{1}H NMR ($CDCl_3$; δ, ppm): 7.94 (m, 22 H, Ar), 7.29 (m, 36 H, Ar), 7.10 (m, 23 H, Ar), 5.15 (m, 20 H), 4.12 (m, 15 H), 0.6–3.0 (m, 65 H).

For $C_{200}H_{181}N_{12}O_2F_4Ir$		
anal. calcd., %:	C, 78.67;	H, 5.99.
Found, %:	C, 78.59;	H, 6.05.

M_w = 45000, M_n = 33700, M_w/M_n = 1.3, T_g = 176°C, T_d = 229°C (at 5% mass loss).

Synthesis of P3 from compounds **I** (0.0389 g, 0.0375 mmol) and **IV** (0.1020 g, 0.3549 mmol) was similar to the procedure described for P1. The copolymerization time was 2.5 h. The yield was 0.12 g (80%).

IR (ν, cm^{-1}): 3125 ν(C=C–H); 3060 ν, 1074, 1035, 1009 δ, 852 γ(C_{Ar}–H); 2953 ν(C–H), 1402 δ_s(C_{Alk}–H); 1604, 1376 ν(C···O); 1602, 1488 ν(C=C_{Ar}); 1577, 1536 ν(pyrazole ring); 1266, 1157 ν(C–F); 970 δ(C=C), 754 δ(C=C–H); 704 δ, 621 ν(chelate ring); 512, 461 ν(Ir–O). ^{1}H NMR ($CDCl_3$; δ, ppm): 7.94 (m, 44 H, Ar), 7.15 (m, 37 H, Ar), 5.16 (m, 20 H), 0.6–4.0 (m, 64 H).

For $C_{200}H_{165}N_{12}O_{10}F_4Ir$		
anal. calcd., %:	C, 75.89;	H, 5.27.
Found, %:	C, 75.78;	H, 5.29.

M_w = 46900, M_n = 32900, M_w/M_n = 1.4, T_g = 170°C, T_d = 368°C (at 5% mass loss).

Synthesis of P4 from compounds **I** (0.0455 g, 0.0439 mmol) and **V** (0.1030 g, 0.3584 mmol) was similar to the procedure described for P1. The copolymerization time was 4.5 h. The yield was 0.12 g (81%).

IR (ν, cm^{-1}): 3125 ν(C=C–H); 3060 ν, 1074, 1035, 1009 δ, 852 γ(C_{Ar}–H); 2944 ν(C–H), 1402 δ_s(C_{Alk}–H); 1604, 1376 ν(C···O); 1602, 1488 ν(C=C_{Ar}); 1577, 1536 ν(pyrazole ring); 1275, 1157 ν(C–F); 970 δ(C=C), 754 δ(C=C–H); 701 δ, 621 ν(chelate ring); 512, 461 ν(Ir–O). ^{1}H NMR ($CDCl_3$; δ, ppm): 7.92 (m, 46 H, Ar), 7.15 (m, 35 H, Ar), 5.14 (m, 20 H), 0.6–4.0 (m, 64 H).

For $C_{200}H_{165}N_{12}O_{10}F_4Ir$		
anal. calcd., %:	C, 75.89;	H, 5.27.
Found, %:	C, 75.80;	H, 5.34.

M_w = 45800, M_n = 34500, M_w/M_n = 1.3, T_g = 186°C, T_d = 363°C (at 5% mass loss).

X-ray diffraction analysis. The crystallographic data for compound **I** were collected on a Smart Apex automated diffractometer (MoK_α radiation, graphite monochromator). The structure was solved by a direct method followed by full-matrix least squares for F^2 using the known program [15]. An absorption correction was applied using the SADABS program [16]. All non-hydrogen atoms were refined in the anisotropic approximation. Hydrogen atoms were placed in geometrically calculated positions and refined in the riding model. In crystal **I**, the norbornene fragment is disordered over two positions, and CH_2Cl_2 molecules are also disordered. The crystallographic characteristics and the main refinement parameters are presented in Table 1.

The crystallographic information for compound **I** was deposited with the Cambridge Crystallographic Data Centre (CCDC 1050692; deposit@ccdc.cam.ac.uk or http://www.ccdc.cam.ac.uk).

Fabrication of OLED devices. A glass plate with the deposited ITO layer (120 nm, 15 Ohm/cm^2) (Lum Tec) acting as an anode served as a support for OLED devices with the configuration ITO/Ir polymer (40 nm)/BATH (30 nm)/Alq_3 (30 nm)/Yb (150 nm). The emission layer of the copolymer was deposited

from its solution in CH_2Cl_2 (5 mg/mL) on a Spincoat G3-8 centrifuge (3000 rpm, 30 s) and dried in vacuo at 70°C for 3 h. The layer thickness was determined with a META-900 ellipsometer. A hole-blocking layer of BATH, an electron-transporting layer of Alq_3, and an Yb layer acting as a cathode were deposited by vacuum (10^{-6} mm Hg) evaporation from separated thermoresistant evaporators. The thickness of the layers was monitored with a calibrated quartz resonator. The active surface area of the devices was a circle with a diameter of 5 mm.

RESULTS AND DISCUSSION

The cyclometallated iridium complex (I) was synthesized by the reaction of dimeric iridium chloride with norbornene-containing sodium pyrazolonate (Scheme 1)

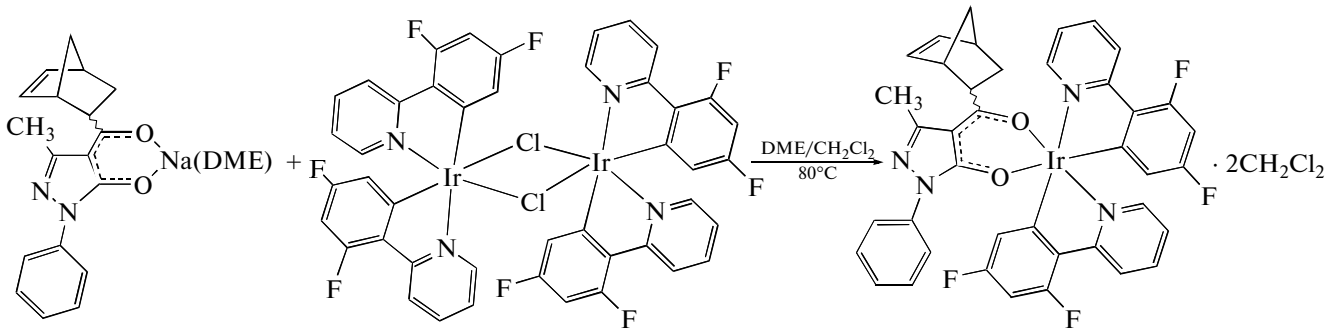

(NBEPz)Na(DME) $[Ir(Dfppy)_2(Cl)]_2$ **(I)**

Scheme 1.

Compound **I** was obtained in a high yield as a yellow crystalline substance stable in air and soluble in chloroform, CH_2Cl_2, and DME. The NMR studies showed that the product was a mixture of *endo* and *exo* isomers in a ratio of 66 : 34.

The structure of complex **I** was determined by X-ray diffraction analysis. The studied single-crystal sample contains only the *endo* isomer (Fig. 1, Table 2).

The iridium atom has a distorted octahedral coordination. The O(1), O(2), C(11), and C(22) atoms lie in the base of the octahedron, and the N(1) and N(2) atoms occupy the axial positions (angle N(1)Ir(1)N(2) 176.3(1)°). The shift of the Ir(1) atom from the plane of the base is 0.015 Å. The lengths of Ir–C (1.987(3), 2.004(4) Å), Ir–N (2.041(3) Å), and Ir–O (2.142(2), 2.152(2) Å) bonds in compound **I** almost coincide with similar distances in the earlier studied related complex ((NBEPz)Ir$(Ppy)_2$) (VI) [17]. It is seen that the presence of the fluorine atoms in the phenylpyridyl ligands in compound **I** does not result in noticeable changes in the geometric characteristics around the iridium atoms compared to complex **VI**.

The phenyl substituent at the N(3) atom in complex **I** is approximately coplanar to the pyrazole fragment N(3,4)C(24–26). The corresponding dihedral angle (5.0°) is substantially smaller than a similar value in **VI** (50.0°). Possibly, such a significant change in this parameter is related to differences in crystal packings of complexes **I** and **VI**. The phenylenepyridine substituents in complex **I** are planar. The dihedral angles between the planes of the pyridine and phenylene fragments (4.8° and 2.1°) are comparable with similar values in structure **VI** (0.68° and 2.55°).

An analysis of the crystal packing of complex **I** shows that the phenyl fragments with the F(3) and F(4) fluorine atoms of the difluorophenylpyridine ligands are parallel to each other and partially overlapped (Fig. 2).

The interplanar distance between the six-membered rings *A* and *B*, *C* and *D* is 3.46 Å. The C(19) atom of the *A* ring is located almost above the center of the adjacent six-membered ring *B* (Fig. 2) at a distance of 3.468(5) Å. The distance between the centers of the *A* and *B*, *C* and *D* rings is 3.80 Å. The found geometric characteristics are comparable with similar characteristics of related compounds Ir$(Dfppy)_2$(DBM) (**VII**) (DBM is dibenzylidenemethane) [18], Ir$(Ppy)_2(L^1)$ (**VIII**) (L^1 is 1-phenyl-3-methyl-4-benzoyl-5-pyrazolone) [19], and Ir$(Ppy)_2(L^2)$ (**IX**) (L^2 is 2'-hydroxyacetophenone) [20], indicating that the crystals of complex **I** and compounds **VII–IX** contain intermolecular

π–π interactions between the difluorophenylpyridyl ligands.

It is known that the inclusion of carbazole groups into the polymer emitters improves their charge transport properties and electroluminescence characteristics [21, 22]. Therefore, the carbazole comonomers **(II–V)** with different structures were used for the preparation of the iridium-containing copolymers. Copolymerization reactions occur in the presence of the Grubbs catalyst of the third generation at room temperature and afford iridium-containing copolymers P1–P4 (Scheme 2)

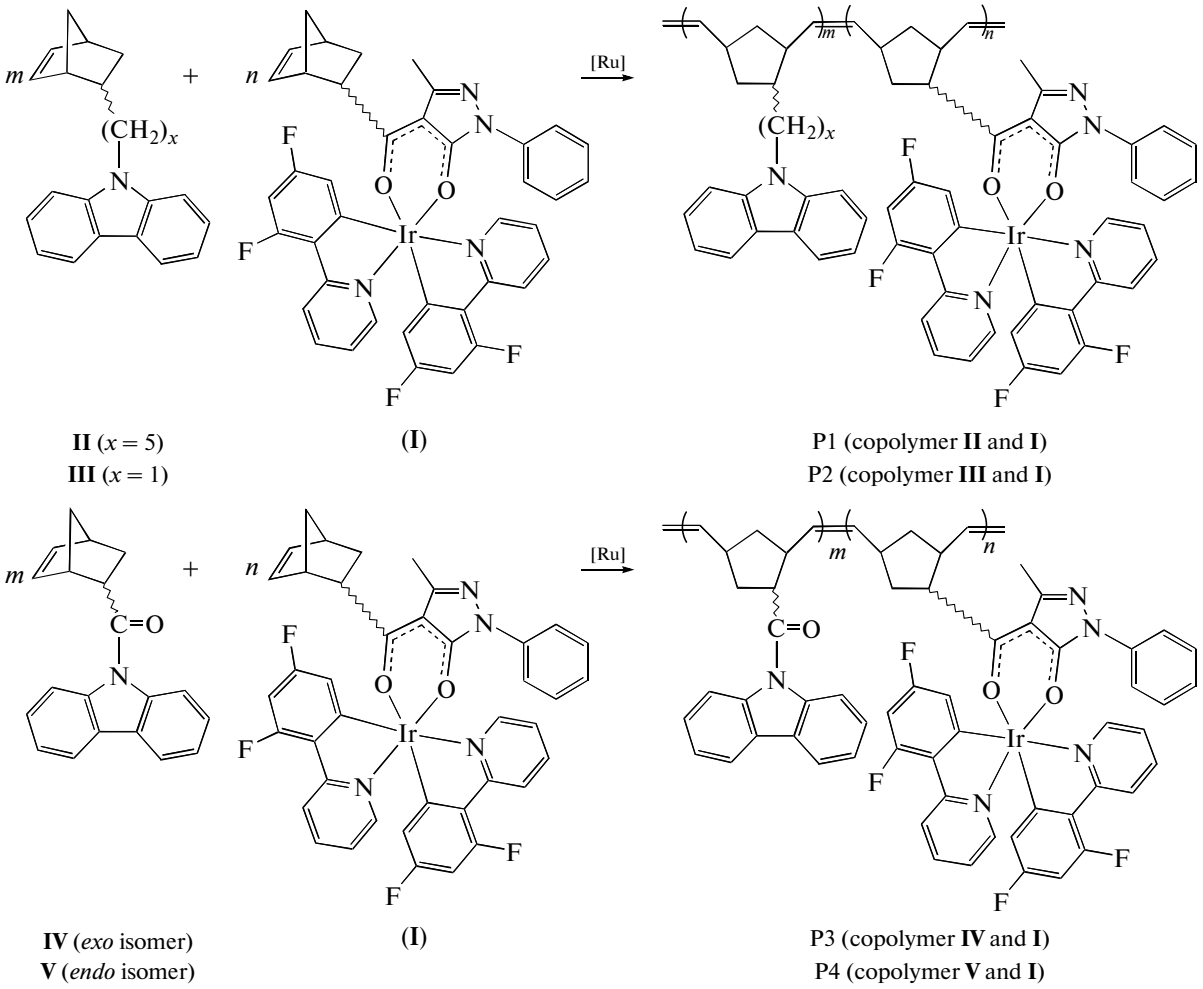

Sheme 2.

In all cases, the initial ratio of the carbazole- and iridium-containing comonomers *m : n* was 8 : 1. The Grubbs catalyst was used in an amount of 1 mol % to the overall amount of comonomers introduced into the reaction. The reaction time was monitored by TLC. The copolymerization of iridium-containing monomer **I** with comonomers **II** and **III** occurs within 2–2.5 h. The reaction involving comonomer **IV** completes within 2.5 h, whereas the copolymerization with less reactive comonomer **V** occurs within 4.5 h. Copolymers P1–P4 were isolated as yellow powders stable in air and highly soluble in THF, CH_2Cl_2, and $CHCl_3$.

The study of the photophysical properties of the synthesized compounds shows that the absorption spectrum of complex **I** (Fig. 3, Table 3) is similar to the spectrum of the known acetylacetonate iridium(III) complex $Ir(Dfppy)_2(Acac)$ [23].

The intense broad band with a maximum at 254 nm in the spectrum of complex **I** is attributed to intraligand $^1(\pi \rightarrow \pi^*)$ transitions in the 2,4-difluorophenylpyridyl and pyrazolonate ligands. The weak bands in a range of 335–500 nm can be assigned to metal-to-ligand charge-transfer (MLCT) transitions mixed with triplet ligand-centered (^{3}LC) transitions [23, 24]. In addition to the bands characteristic of complex **I**, the absorption spectra of copolymers P1–P4 contain additional intense bands in a range of 260–345 nm

induced by the $\pi \rightarrow \pi^*$ transitions in the carbazole fragments.

The PL spectrum of complex **I** (Fig. 4) in a CH_2Cl_2 solution contains a band with a maximum at 485 nm assigned to the ^{3}LC transitions [23–25] and a lower-intensity band at 506 nm (shoulder to the main band), which can be ascribed (by analogy to published data [24]) to the ^{3}MLCT transitions. In the PL spectrum of the crystalline sample (Fig. 4), the intermolecular $\pi-\pi$ transitions result in the redistribution of intensities of the emission bands, the band corresponding to the ^{3}MLCT transitions is the main, and a band at 555 nm appears (shoulder to the main band) that can be attributed to the ^{3}MLLCT transitions [18].

The PL spectra of copolymers P1–P4 in a solution and in thin films (Fig. 5, Table 3) contain intense broad bands with maxima in a range of 480–515 nm assigned to the ^{3}LC and ^{3}MLCT transitions in the cyclometallated iridium complexes and lower-intensity bands in a range of 375–460 nm characteristic of excimers of carbazole groups [26]. The presence of the emission bands of the carbazole groups in the spectra indicates an incomplete transfer of the excitation energy from the polymer matrix to the luminophore iridium complexes via the Förster mechanism [27].

The PL quantum yields of copolymers P1–P4 are considerably higher than the quantum yield of complex **I** (Table 3). This is probably related to the fact that the iridium-containing fragments in the macromolecules are noticeably shielded by the carbazole groups and, hence, their interaction with the solvent leading to nonradiative losses is hindered. The structures of the carbazole-containing units also exert a substantial effect on the PL efficiency of the synthesized copolymers. The quantum yields of P3 and P4 exceed the corresponding values for polymer emitters P1 and P2 (Table 3). It can be assumed that the carbazole groups bound to the polymer chains by the carbonyl bridges (copolymers P3 and P4) are less mobile and their aggregation and excimer formation are less probable than in copolymers P1 and P2. Therefore, the transfer of the excitation energy from the carbazole fragments to the iridium complexes in emitters P3 and P4 is more efficient, which is manifested as higher quantum yields, compared to that for emitters P1 and P2.

The EL properties of copolymers P1–P4 were studied for model OLED devices with the configuration ITO/Ir copolymer (40 nm)/BATH (30 nm)/Alq_3 (30 nm)/Yb. The EL spectra of polymers P1–P4 and the working characteristics of the related OLED devices are presented in Figs. 6 and 7 and in Table 4.

The EL spectra of copolymers P1–P4 are similar and contain bands with maxima at 490–520 nm assigned to the ^{3}LC/^{3}MLCT transitions in the cyclometallated iridium complexes bound to the polymer

Table 1. Crystallographic data and the X-ray diffraction experimental and refinement parameters for complex **I**

Parameter	Value
FW	1037.74
Temperature, K	100(2)
Crystal system	Triclinic
Space group	$P\bar{1}$
a, Å	11.7175(6)
b, Å	13.1595(7)
c, Å	13.5149(8)
α, deg	91.209(1)
β, deg	109.798(1)
γ, deg	90.741(1)
V, Å^3	1959.89(19)
Z	2
F(000)	1024
ρ_{calcd}, g/cm^{-3}	1.758
μ, mm^{-1}	3.742
Crystal size, mm	0.25 × 0.15 × 0.12
Measurement range θ, deg	1.85–26.00
Ranges of reflection indices	$-14 \le h \le 14$, $-15 \le k \le 16$, $-16 \le l \le 10$
Number of reflections	11622
Number of independent reflections	7619
R_{int}	0.0185
GOOF (F^2)	1.033
R_1, wR_2 ($I > 2\sigma(I)$)	0.0370, 0.0904
R_1, wR_2 (for all parameters)	0.0475, 0.0945
$\Delta\rho_{max}/\Delta\rho_{min}$, *e* Å^{-3}	1.580/–1.147

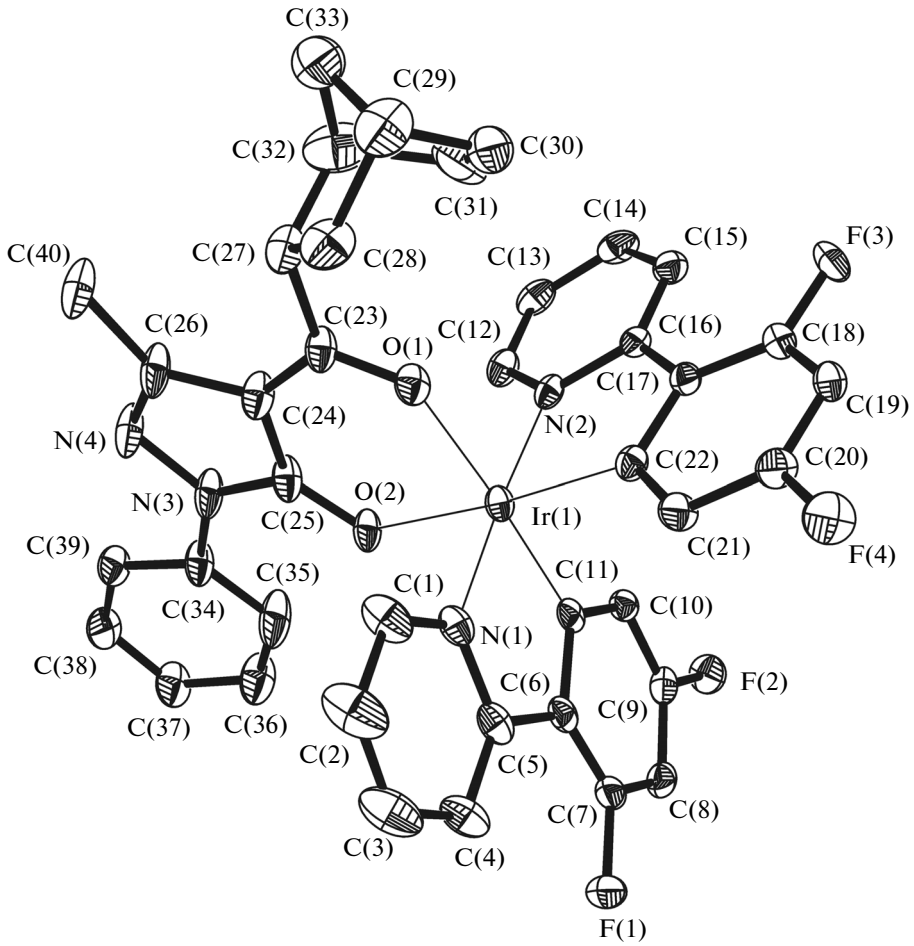

Fig. 1. Molecular structure of complex **I**. Thermal ellipsoids are presented with 30% probability. Molecules of crystallization CH_2Cl_2 are omitted.

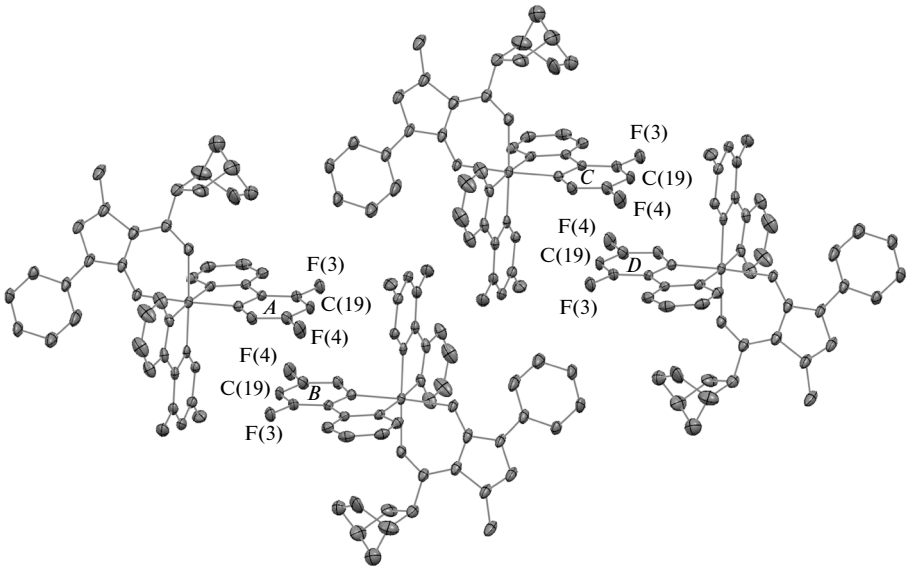

Fig. 2. Fragment of the crystal packing of complex **I**. Thermal ellipsoids are presented with 30% probability. Hydrogen atoms are omitted.

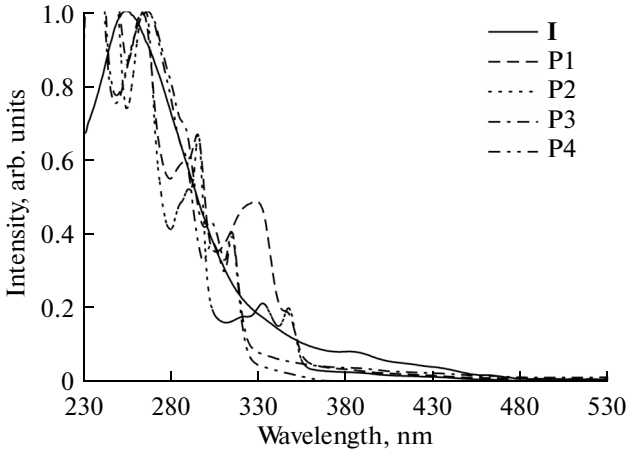

Fig. 3. Absorption spectra of complex **I** and copolymers P1–P4 in a CH_2Cl_2 solution.

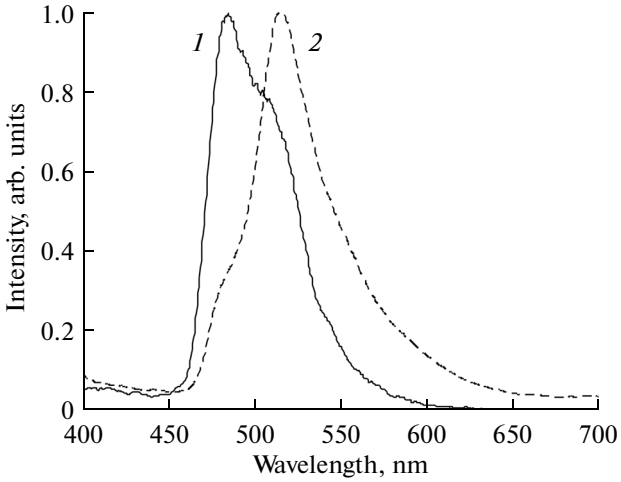

Fig. 4. Photoluminescence spectra of complex **I** in (*1*) a CH_2Cl_2 solution and (*2*) crystals at room temperature ($\lambda_{exc} = 360$ nm).

Table 2. Selected bond lengths (Å) and bond angles (deg) in complex **I**

Bond	*d*, Å	Angle	ω, deg
Ir(1)–O(1)	2.142(2)	C(22)Ir(1)C(11)	91.0(1)
Ir(1)–O(2)	2.152(2)	C(22)Ir(1)N(2)	80.7(1)
Ir(1)–N(1)	2.041(3)	C(11)Ir(1)N(2)	96.5(1)
Ir(1)–N(2)	2.041(3)	C(22)Ir(1)N(1)	96.7(1)
Ir(1)–C(11)	1.987(3)	C(11)Ir(1)N(1)	80.9(1)
Ir(1)–C(22)	2.004(4)	N(2)Ir(1)N(1)	176.3(1)
O(1)–C(23)	1.270(4)	C(22)Ir(1)O(1)	90.4(1)
O(2)–C(25)	1.291(4)	C(11)Ir(1)O(1)	176.1(1)
N(1)–C(1)	1.353(5)	N(2)Ir(1)O(1)	87.3(1)
N(1)–C(5)	1.372(5)	N(1)Ir(1)O(1)	95.4(1)
N(2)–C(12)	1.354(5)	C(22)Ir(1)O(2)	174.4(1)
N(2)–C(16)	1.374(5)	C(11)Ir(1)O(2)	91.0(1)
N(3)–C(25)	1.368(5)	N(2)Ir(1)O(2)	93.9(1)
N(3)–N(4)	1.391(4)	N(1)Ir(1)O(2)	88.8(1)
N(3)–C(34)	1.434(5)	O(1)Ir(1)O(2)	87.9(1)
N(4)–C(26)	1.323(5)	O(1)C(23)C(27)	115.6(3)
C(24)–C(26)	1.471(5)	O(2)C(25)N(3)	121.7(3)
C(30)–C(31)	1.339(4)	C(25)N(3)C(34)	129.7(3)
C(23)–C(24)	1.419(6)		
C(24)–C(25)	1.427(5)		

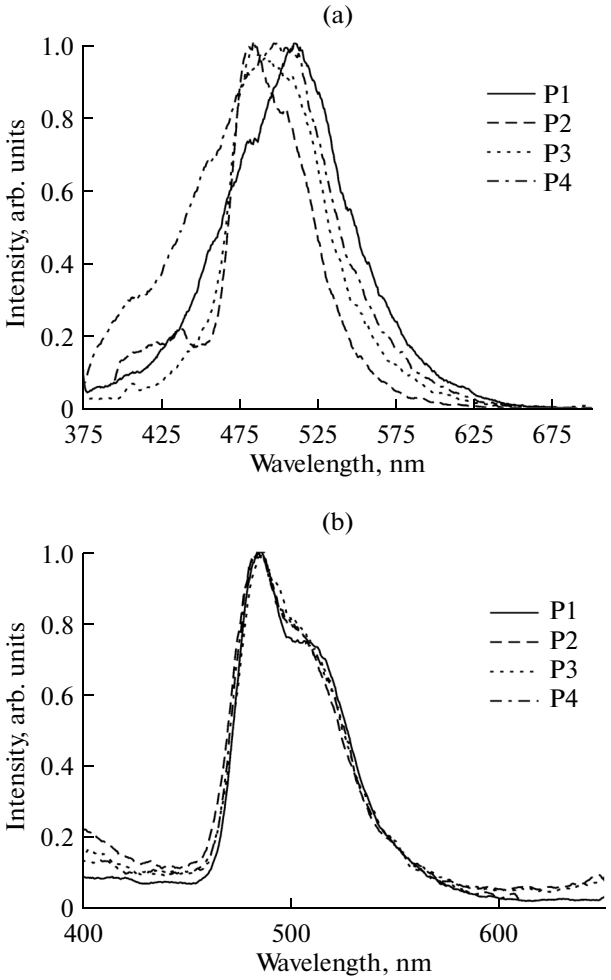

Fig. 5. Photoluminescence spectra of copolymers P1–P4 in (a) solutions and (b) thin films at room temperature (λ_{exc} = 360 nm).

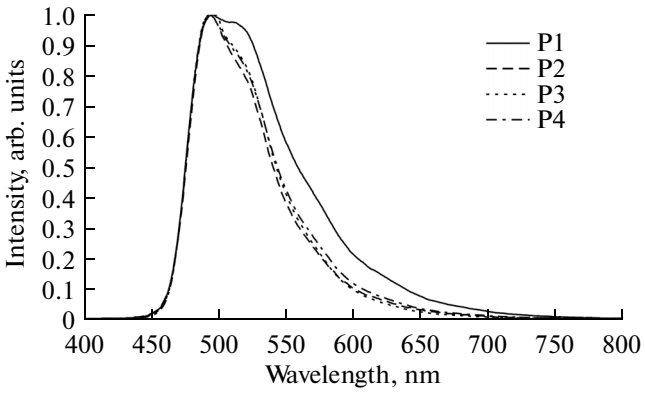

Fig. 6. Normalized EL spectra of copolymers P1–P4.

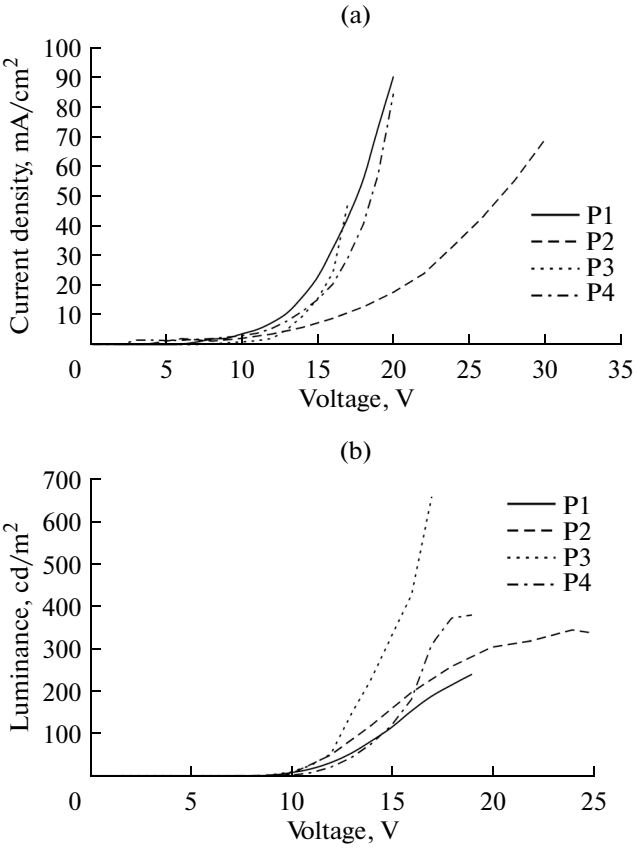

Fig. 7. (a) Current density-voltage and (b) luminance-voltage characteristics of the OLEDs based on polymers P1–P4.

chain. The absence of the emission of the carbazole groups indicates the efficient transfer of the excitation energy from the polymer matrix to the iridium-containing fragments via the Förster mechanism [27]. The chromaticity coordinates of the radiation of the OLEDs in the CIE (Commision Internationale de l'Eclairage) diagram (Table 4) correspond to the green color and remain nearly unchanged in the whole range of working voltages. The highest EL characteristics were shown by the OLED based on copolymer P4 (Table 4).

Thus, the new iridium-containing norbornene monomer **I** was synthesized, and the new carbochain copolymers P1–P4 with carbazole and iridium-containing fragments in the side chains were obtained from this monomer using the ROMP method. The obtained polymer emitters exhibit the intense green PL and EL. The maximum values of EL luminance (655 cd/m^2), current efficiency (2.60 cd/A), and power efficiency (0.63 Lm/W) were reached using emitter P3.

Table 3. Photophysical characteristics of complex **I** and polymers P1–P4

Compound	λ_{abs}/log ε	λ_{em}, nm		Quantum yield, % (in CH_2Cl_2)
		film	CH_2Cl_2	
I	254 (4.67), 335 sh (3.87), 384 (3.56), 410 sh (3.35), 430 sh (3.24), 460 sh (2.87)	485 sh, 516, 555 sh (in crystals)	485, 506 sh	0.7
P1	263 (5.54), 285 sh (5.30), 289 sh (5.32), 295 (5.38), 322 sh (5.21), 330 (5.22), 346 (4.82), 365 sh (4.14), 380 sh (4.04), 412 sh (3.81), 428 sh (3.72), 457 sh (3.47)	486, 506 sh	485 sh, 511	1.9
P2	265 (5.16), 2.85 sh (5.12), 289 sh (5.29), 295 (4.72), 320 sh (4.80), 332 (4.77), 347 (4.77), 370 sh (3.90), 383 sh (3.85), 412 sh (3.62), 435 sh (3.51), 458 sh (3.07)	484, 504 sh	484, 508 sh	7.8
P3	266 (5.33), 286 sh (5.18), 303 (4.97), 314 (4.94), 344 sh (4.09), 367 sh (3.93), 383 sh (3.89), 406 sh (3.75), 433 sh (3.65), 457 sh (3.47), 484 sh (3.31)	486, 503 sh	484, 507 sh	16.8
P4	266 (5.36), 286 sh (5.17), 303 (4.95), 314 (4.97), 344 sh (4.02), 367 sh (3.72), 383 sh (3.66), 406 sh (3.42), 433 sh (3.22), 457 sh (2.63)	484, 502 sh	484 sh, 499	19.1

Table 4. Working characteristics* of the light diodes based on copolymers P1–P4

Ir polymer	Turn-on voltage, V**	Maximum luminance, cd/m^2	Maximum current efficiency, cd/A	Maximum power efficiency, Lm/W	Chromaticity coordinates in CIE diagram
P1	9	239 (19 V)	0.53 (16 V)	0.12 (13 V)	$x = 0.22$ $y = 0.50$
P2	14	343 (24 V)	2.15 (16 V)	0.44 (14 V)	$x = 0.17$ $y = 0.49$
P3	9	655 (17 V)	2.60 (13 V)	0.63 (13 V)	$x = 0.16$ $y = 0.50$
P4	10	378 (19 V)	1.04 (17 V)	0.19 (17 V)	$x = 0.17$ $y = 0.49$

* The voltage at which the working characteristics were determined is given in parentheses.

** Luminance at 1 cd/m^2.

ACKNOWLEDGMENTS

This work was supported by the Russian Foundation for Basic Research (project no. 15-43-02178-r_povolzh'e_a) and the Ministry of Education and Science of the Russian Federation (project no. 02.V.49.21.0003).

REFERENCES

1. *Highly Efficient OLEDs with Phosphorescent Materials*, Yersin, H., Ed., Weinheim: Wiley–VCH, 2008, p. 456.
2. Happ, B., Winter, A., Hager, M.D., and Schubert, U.S., *Chem. Soc. Rev.,* 2012, vol. 41, p. 2222.
3. Zhao, Q., Liu, S.-J., and Huang, W., *Macromol. Rapid. Commun.,* 2010, vol. 31, p. 794.
4. Choi, M.-C., Kim, Y., and Ha, C.-S., *Prog. Polym. Sci.*, 2008, vol. 33, p. 581.
5. Marin, V., Holder, E., Hoogenboom, R., and Schubert, U.S., *Chem. Soc. Rev.*, 2007, vol. 36, p. 618.
6. Shunmugam, R. and Tew, G.N., *Macromol. Rapid Commun.*, 2008, vol. 29, p. 1355.
7. Sakai, H., Itaya, A., Masuhara, H., et al., *Polymer*, 1996, vol. 37, p. 31.
8. Begantsova, Y.E., Bochkarev, L.N., Malysheva, I.P., et al., *Synth. Met.*, 2011, vol. 161, p. 1043.
9. Meyers, A., Kimyonok, A., and Weck, M., *Macromolecules*, 2005, vol. 38, p. 8671.
10. Liaw, D.-J. and Tsai, C.-H., *Polymer*, 2000, vol. 41, p. 2773.
11. Rozhkov, A.V., Bochkarev, L.N., Basova, G.V., et al., *Russ. J. Gen. Chem.*, 2012, vol. 82, no. 12, p. 1895.
12. Love, J.A., Morgan, J.P., Trnka, T.M., and Grubbs, R.H., *Angew. Chem., Int. Ed. Engl.*, 2002, vol. 41, p. 4035.
13. Magde, D., Wong, R., and Seybold, P.G., *Photochem. Photobiol.*, 2002, vol. 75, p. 327.
14. Demas, J.N. and Crosby, G.A., *J. Phys. Chem.*, 1971, vol. 75, p. 991.
15. Sheldrick, G.M., *SHELXTL. Version 6.12. Structure Determination Software Suite*, Madison: Bruker AXS, 2000.
16. Sheldrick, G.M., *SADABS. Version 2.01. Bruker/Siemens Area Detector Absorption Correction Program*, Madison: Bruker AXS, 1998.
17. Begantsova, Yu.E., Bochkarev, L.N., Samsonov, M.A., et al., *Russ. J. Coord. Chem.*, 2013, vol. 39, no. 9, p. 661.
18. Shin, C.H., Huh, J.O., Lee, M.H., and Do, Y., *Dalton Trans.*, 2009, p. 6476.
19. Wu, H., Yang, T., Zhao, Q., et al., *Dalton Trans.*, 1969, vol. 40, p. 1969.
20. Huang, K., Wu, H., Shi, M., et al., *Chem. Commun.*, 2009, p. 1243.
21. Grimsdale, A.C., Chan, K.L., Martin, R.E., et al., *Chem. Rev.*, 2009, vol. 109, p. 897.
22. Bochkarev, M.N., Vitukhnovskii, A.G., and Katkova, M.A., *Organicheskie svetoizluchayushchie diody (OLED)* (Organic Light-Emitting Diodes (OLEDs)), Nizhny Novgorod: Dekom, 2011.
23. Liu, Z., Nie, D., Bian, Z., et al., *Chem. Phys. Chem.*, 2008, vol. 9, p. 634.
24. Rausch, A.F., Homeier, H.H.H., and Yersin, H., *Top. Organomet. Chem.*, 2010, vol. 29, p. 193.
25. Li, J., Djurovich, P.I., Alleyne, B.D., et al., *Inorg. Chem.*, 2005, vol. 44, no. 6, p. 1713.
26. Sakai, H., Itaya, A., Masuhara, H., et al., *Polymer*, 1996, vol. 37, p. 31.
27. Förster, T., *Disc. Faraday Soc.*, 1959, vol. 27, p. 7.

Translated by E. Yablonskaya